Investigating the Distribution of Potassium Perfluoro (2-Ethoxyethane) Sulfonic Acid in Water/Gas Systems using Molecular Dynamics Method

Xianwu Jing,[1,2,*] Qiang Wang,[3] Long Xian,[4] Zeyin Jiang,[1] Xin Huang[1]

[1] Research Institute of Natural Gas Technology, PetroChina Southwest Oil and Gasfield, Chengdu, Sichuan, 610213, People's Republic of China

[2] Shale Gas Evaluation and Exploitation Key Laboratory of Sichuan Province, Sichuan Provincial Department of Science and Technology, Chengdu, Sichuan, 610051, People's Republic of China

[3] Engineering Technology Department, PetroChina Southwest Oil and Gasfield Company, Chengdu, Sichuan, 610057, People's Republic of China

[4] Chengdu Pidu Xingneng Co., Ltd, Sichuan Huayou Group Co., Ltd, Chengdu, Sichuan 611730, People's Republic of China

* Corresponding author's e-mail address: jingxw2018@petrochina.com.cn

Abstract: Molecular dynamics method (MD) was used to study the distribution of potassium perfluoro (2-ethoxyethane) sulfonic acid (PESK) in water/gas systems. During the MD process, PES$^-$ spontaneously moves to the water surface, which is also the principle by which surfactants act. At equilibrium, most of the fluorocarbon chain faces the gas phase while the sulfonic acid radical faces the water, with a very small quantity of PES$^-$ and K$^+$ is still in the bulk solution. The distribution of quantity density and charge density both confirm that PES$^-$ is mainly distributed at the water/gas interface. Weak intermolecular interactions were analyzed using the IGMH method, with the main interaction energy between PES$^-$ and water coming from h-bonds formed by the oxygen atom in the sulfonic acid group and hydrogen atom in water molecules. There is only van der Waals interaction between K$^+$ and H$_2$O molecules. The strength of the interaction between surfactants and water molecules was studied through energy decomposition.

Keywords: fluorocarbon surfactant, molecular dynamics simulation, IGMH, LUMO, HOMO, electrostatic potential.

INTRODUCTION

IN recent years, there has been an increasing challenge in the development of oil and gas resources,[1] especially in the context of shale gas or shale oil reserves.[2] Hydraulic fracturing is widely recognized as a highly effective method for enhancing gas and oil production. This technique involves the injection of a substantial volume of liquid, typically water, along with quartz sand or ceramsite, known as proppant, into the geological formation. The injected fluid creates numerous small fractures within the formation, and upon extraction, the proppant remains within these fractures. This process serves to expand the seepage areas for gas and oil, ultimately leading to increased production levels.[3,4] The liquid typically does not naturally seep back into the ground, necessitating the addition of drainage aids.[5,6]

Surfactants are extensively utilized in the gas/oil industry for a multitude of applications, such as enhanced oil recovery (EOR), drilling, fracturing, acidizing, et al.[7–9] Surfactants incorporating fluorinated hydrocarbons exhibit remarkable thermal, salt, and chemical resistance, rendering them the optimal selection for applications characterized by high temperatures and mineral concentrations.[10–12] Therefore, it is necessary to study, fluorinated surfactant monomers and interfacial structures.[13] Molecular dynamic simulation (MD) helps understand how fluorosurfactants work by studying the small-scale interactions between molecules and surfaces. Using molecular simulations, Jang et al.[14] studied the interfacial tension of cetylbenzenesulfonate with benzenesulfonic acid groups at various positions. Additionally, Wardle et al.[15] studied how surfactants affect the movement of sodium ions in mixtures containing inorganic salts, water, and hexanol.

Research is currently focused on novel fluorine-containing surfactants with unique structures that are not easily accessible. Potassium perfluoro (2-ethoxyethane) sulfonate (PESK) has attracted attention as a surfactant (CAS No. 117205-07-9, also known as PESK).[16] In this study, molecular dynamics simulation method was used to investigate examine PESK distribution on the surface of an aqueous solution.

COMPUTATIONAL DETAILS

The calculation details were as follows:[17] as a first step, ORCA version 5.0.4[18,19] was adopted to optimize the structure of PES$^-$ using B97-3c method,[20] the optimized molecular structure formula is shown in Figure 1. Then the single point energy was calculated by using the theoretical method of B3LYP D3 def2-TZVP.[21] The MD simulation was performed using GROMACS version 2019.6 software,[22,23] GAFF[24] force filed was used to describe PES$^-$, the RESP charge[25] was calculated by using Multiwfn.[26] Then, packmol[27] was used to construct the box as shown in Figure 2A; the OPC three-point model was used to describe water.[28] In the current work, the simulation box contains 100 PES$^-$, 100 K$^+$, and 32862 water molecules, resulting in a PESK concentration of approximately 166 mmol L^{-1}. The box size ($X \times Y \times Z$) is $10 \times 30 \times 10$ nm, the solution inside the box is $10 \times 10 \times 10$ nm. After energy minimization using the steepest descent algorithm, 200 ns MD was carried out under NVT ensemble. V-rescale algorithm[29] was employed and coupling constant time was 0.2 ps. The PME algorithm[30] was used to calculate Coulomb interaction, and the van der Waals interaction algorithm was cut-off. Visual observation was conducted using VMD software.[31]

IGMH analysis steps are as follows: firstly, all atoms/molecules within 3.5 nm of an specific atom/molecule are selected; secondly, wavefunction information is obtained by ORCA with B3LPY D3 ma-def2-TZVP; thirdly, Multiwfn is used for IGMH analysis.[32]

RESULTS AND DISCUSSION

Solution State Before and After MD

The solution state before and after MD are quit different. As shown in Figure 2A, before the MD starts, K$^+$ and PES$^-$ are both distributed in the bulk solution and the distribution is irregular. When the simulation starts, the PES$^-$ in the solution gradually moves towards the water/gas interface; when the simulation reached 100 ns, the system basically reached equilibrium and there was no PES$^-$ in the bulk solution, as shown in Figure 2C. After the MD is completed, PES$^-$ is mainly distributed at the water/gas interface, as shown in Figure 2E. This is precisely the mechanism by which surfactants reduce surface-tension. This means that at this concentration of 166 mmol L^{-1}, PES$^-$
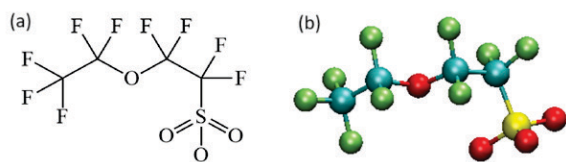

Figure 1. Molecular structure formula of PES$^-$ (a): structural formula; (b): molecular structure of the ball and stick model).

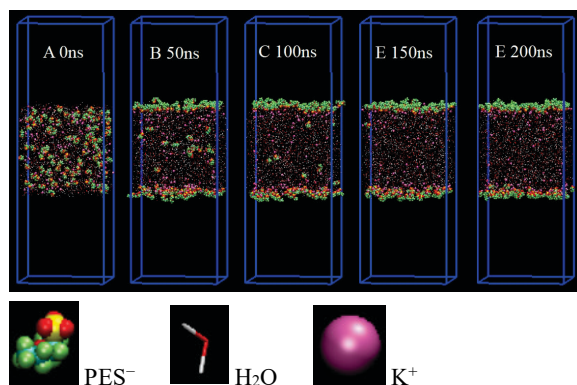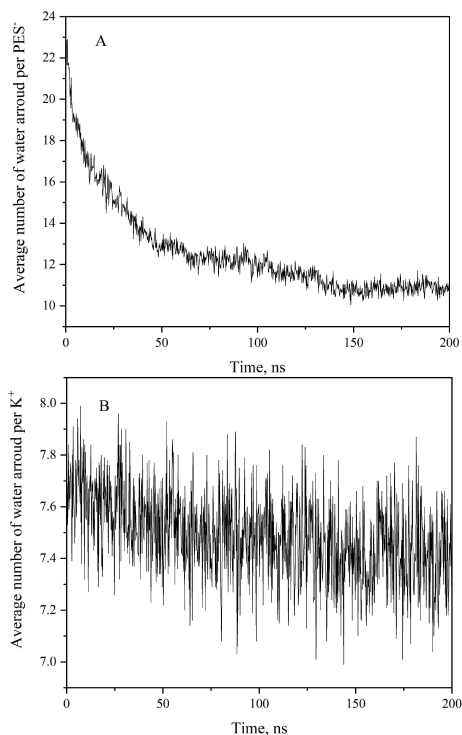**Figure 2.** Snapshots of PESK aqueous solution before and after MD.

Figure 3. Average number of water molecules arroud per PES$^-$ and K$^+$.

can distribute on the water surface. K⁺ is mainly located near PES⁻ and a small quantity of K⁺ are still distributed in bulk aqueous solution randomly without aggregations. The video of the trajectory can be obtained here https://youtu.be/342TqFFzJC4.

It is obvious that the process of PES⁻ spontaneously move from the bulk solution to the water/gas interface, is actually a process of PES⁻ changing from being completely surrounded by water to partially in contact with water. Here, we investigated the average water number of 0.35 nm near each PES⁻ and K⁺.

From Figure 3A, it can be seen that during the simulation process, the number of water molecules around each PES⁻ gradually decreases, indicating that the PES⁻ continues to move towards the water/gas interface. When the simulation reaches approximately 100 ns, there is no significant change, indicating that the simulation has reached totally equilibrium. In Figure 3B, the number of water molecules near K⁺ remains basically unchanged. Combining with Figure 2E, we believe that all PES⁻ in the box is distributed at the water/gas interface and K⁺ is always in the bulk solution.

Radial Distribution Function (RDF) Analysis Between Atoms With Opposite Charges

The radial distribution function (RDF) can describe the configuration of PES⁻ and K⁺. It indicates the position for a given particle α, the probability of particle β appearing. It can be seen in Figure 4 that the RDF between O atom in PES⁻ and K⁺ peaks at 0.28 nm, which is the first coordination layer. There is also a weak peak above 0.43 nm, which is the second coordination layer. The RDF curve (red one) is also very similar to the black one, but it has a much higher peak value than the black curve. As a result of electrostatic attraction, K⁺ and oxygen atoms in water molecules are also located closely, this is because K⁺ is more evenly distributed in the bulk solution than PES⁻, so the peak value is lower and tends to 1.
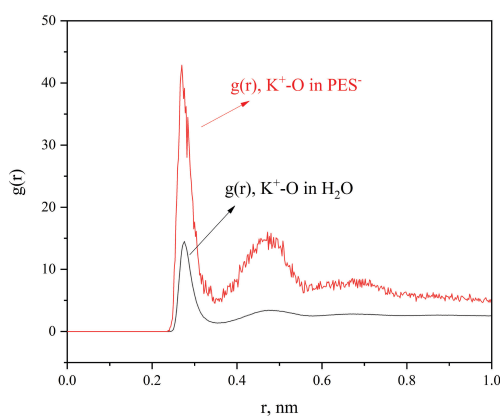
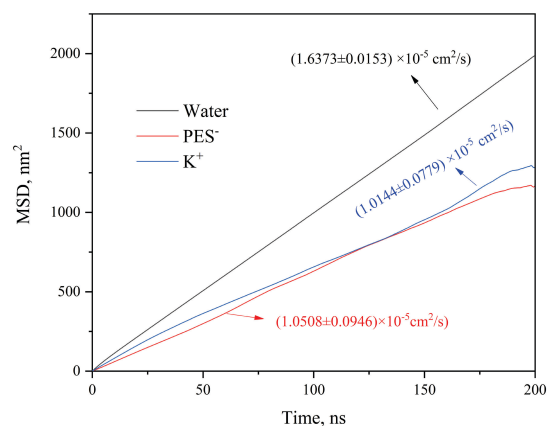**Figure 4.** The RDF of K⁺ between O atoms in PES⁻, and K⁺ between O atoms in water.

Figure 5. MSD of each component of the simulated system.

Mean Square Displacement (MSD) Analysis

In the MD process, particles within the system constantly move, resulting in varying positions at each stage. As a valuable tool for examining the diffusion characteristics of diminutive molecules, the mean square displacement (MSD) measures the average square displacement of these particles. According to Figure 5, the diffusion coefficient of water is $(1.6373 \pm 0.0153) \times 10^{-5}$ cm² s⁻¹, it is observed that this diffusion coefficient is lower than that of the OPC3 water model $(2.28 \pm 0.0020) \times 10^{-5}$ cm² s⁻¹.[28] This disparity can be attributed that PES⁻ molecules have a larger volume and molecular weight than water molecules, thereby impeding the movement of water and reducing its diffusion coefficient in surfactant solutions. The diffusion coefficient of K⁺ is $(1.0144 \pm 0.0779) \times 10^{-5}$ cm² s⁻¹, while the PES⁻ diffusion coefficient is $(1.0508 \pm 0.0946) \times 10^{-5}$ cm² s⁻¹, there is a great deal of similarity between these two values. This disparity can be attributed to the strong electrostatic attraction between positively charged K⁺ and negatively charged PES⁻, they always appear in pairs, resulting in a significantly lower coefficient than that of water.

Number Density Distribution Analysis

An essential aspect of understanding the interaction of PES⁻ and K⁺ ions is their distribution within a solution. PES⁻ are mainly concentrated at the water/gas interface, while K⁺ ions are located near the PES⁻ layer and dispersed throughout the bulk solution. In Figure 6, the number density of both PES⁻ and K⁺ are calculated and plotted to quantify this distribution

As shown in Figure 6A, this observation is consistent with Figure 2A, which shows the PES⁻ solution with an irregular number density in the bulk solution and a number density of 0 per nm³ on both sides (in gasous). Figure 6B shows a number density of approximately 0.45 per nm³ at
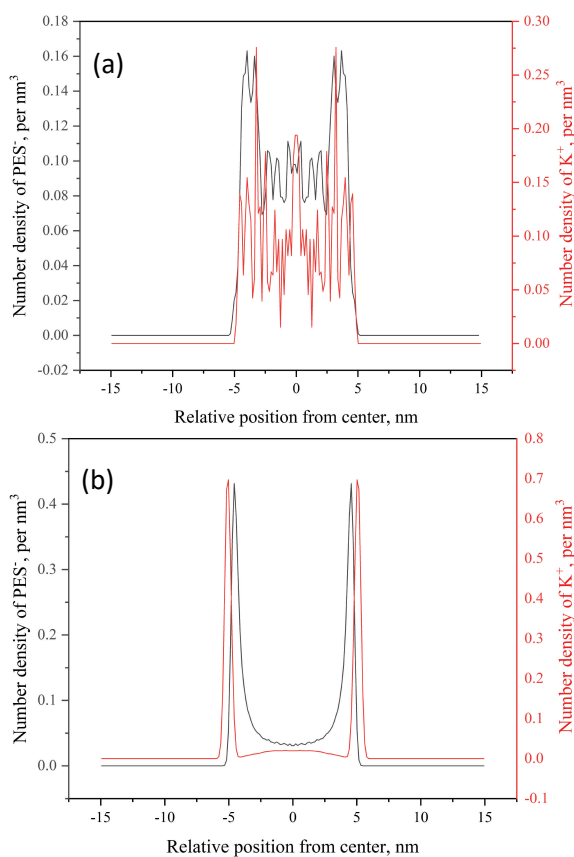
Figure 6. Number density of PES⁻ and K⁺ before and after MD (a) before; (b):after.

Figure 7. IGMH analysis (A: PES⁻ at the water/gas interface with surrounding water molecules/ions; B: K⁺ in bulk solution with surrounding water molecules).

a distance of about 5 nm from the center, in contrast with nearly zero density in bulk solution. In this manner, PES⁻ are primarily gathered at the water/gas interface. Alternatively, K⁺ ions have a density of 12 per nm³ in areas with the most sulfonate groups, suggesting that they are likely to occur near sulfonate groups. This is consistent with the results of RDF.

IGMH Analysis

Here, weak intermolecular interactions were analyzed using the IGMH method. Figure 7 shows two types of weak interactions. Firstly, the blue isosurface in Figure 7A shows H-bonds formed between PES⁻ molecules and adjacent H_2O molecules, blue dots are displayed in the scatter plot at the same time, but some water molecules only have van der Waals interactions with PES⁻. Van der Waals interaction takes place when K⁺ is distributed around PES⁻ molecules, as indicated by the arrow, shown as the green isosurface and displays as green dots in the scatter plot. Because K⁺ is a positively charged atom and oxygen in water is negatively charged, the oppositely charged atoms attract each other, so the coordinate position of water molecules determines
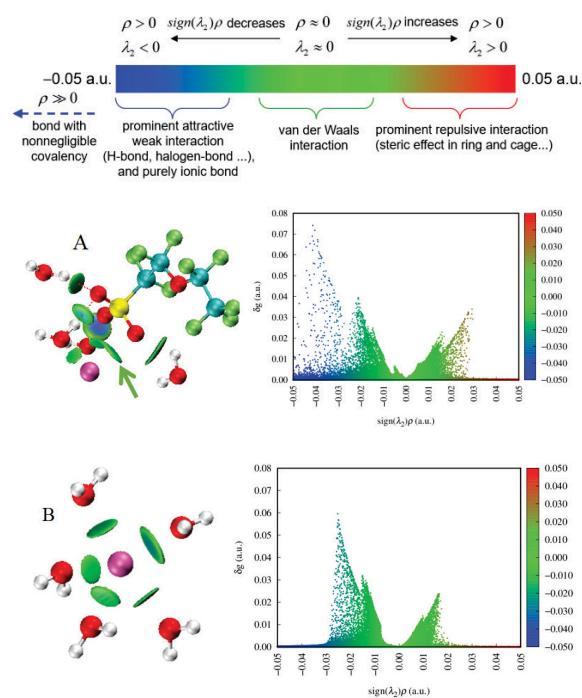
the direction of van der Waals interactions. As shown as the green isosurface in Figure 7B, the scatter plot is filled with green dots instead of blue, indicating that the interaction between K⁺ and water is extremely weak. There is no red isosurface in Figure 6A and 6B, nor is there any red area in the scatter plot, indicating that there is no obvious repulsion between molecules.

CONCLUSION

Using the MD method, the dispersive process of potassium perfluorohexanesulfonate (PESK) in aqueous solution was investigated. Simulation experiments indicate that PES⁻ is distributed spontaneously at the water/gas surface; hydrophilic sulfonic acid groups are immersed in water, while hydrophobic fluorocarbon chains face the gaseous phase. This is also the basic principle of surfactants reducing water surface tension. The distribution of molecular quantity density confirms this conclusion. Due to the attraction of charges, PES⁻ and K⁺ are likely to appear in pairs. K⁺ has only van der Waals interactions with adjacent water molecules, while O atoms in PES⁻ form multiple h-bonds with adjacent water molecules.

REFERENCES

[1]   Y. Wang, Z. Lv, *J. Frontiers in Physics* **2023**, *11*, 1181302.
https://doi.org/10.3389/fphy.2023.1181302

[2]   S. Longde, Z. Caineng, J. Ailin, W. Junsheng, Z. Rukai, W. Sngtao, Z. Guo, *J. Petroleum Exploration and Development* **2019**, *46*, 1073–1087.
https://doi.org/10.1016/S1876-3804(19)60264-8

[3]   L. Qun, X. U. Yun, C. Bo, B. Guan, X. Wang, G. Bi, H. Li, S. Li, B. Ding, H. Fu, Z. Tong, T. Li, H. Zhang, *J. Petroleum Exploration and Development* **2022**, *49*, 191–199.
https://doi.org/10.1016/S1876-3804(22)60015-6

[4]   X. Zheng, S. Junfeng, C. Gang N. Yang, M. Cui, D. Jia, H. Liu, *J. Petroleum Exploration and Development* **2022**, *49*, 644–659.
https://doi.org/10.1016/S1876-3804(22)60054-5

[5]   Y. Zhou, L. You, Y. Kang, K. Li, M. Chen, *J. Geoenergy Science and Engineering*, **2023**, 211437.
https://doi.org/10.1016/j.geoen.2023.211437

[6]   R. K. Saini, B. Crane, N. R. Shimek, W. Wang, B. Cooper, *J. Chem. Eng.* **2022**, *100*, 1309–1322.
https://doi.org/10.1002/cjce.24269

[7]   A. Hassan, M. Mahmoud, B. S. Bageri, M. S. Aljawad, M. S. Kamal, A. A. Barri, I. A. Hussein, *J. Energy & Fuels* **2020**, *34,* 15593–15613.
https://doi.org/10.1021/acs.energyfuels.0c03279

[8]   P. J. Boul, P. M. Ajayan, *J. Energy Technol.* **2020**, *8*, 1901216. https://doi.org/10.1002/ente.201901216

[9]   S. Samsol, P. Pauhesti, H. Pramadhika, M. Z. Abidin, O. Ridaliani, P. Wijayanti, A. Nugrahanti, *Rudarsko-geološko-naftni zbornik* **2023**, *38*, 31–39.
https://doi.org/10.17794/rgn.2023.5.3

[10] J. John, F. Coulon, P. V. Chellam, *J. Water Process Eng.* **2022**, *45*, 102463.
https://doi.org/10.1016/j.jwpe.2021.102463

[11] Y. Lu, Y. Zhu, F. Yang, Z. Xu, Q. Liu, *Advanced Science* **2021**, *8*, 2004082.
https://doi.org/10.1002/advs.202004082

[12] H. Liu, X. Cai, F. Tian F, *Chem. Eng. Oil & Gas* **2022**, *51*, 84–90.
http://dx.doi.org/10.3969/j.issn.1007-3426.2022.06.012

[13] L. Zhang, Z. Liu, T. Ren, P. Wu, J.-W. Shen, W. Zhang, X. Wang, *Langmuir* **2014**, *30,* 13815–13822.
https://doi.org/10.1021/la5030586

[14] S. S. Jang, S. Lin, P. K. Maiti, M. Blanco, W. A. Goddard, P. Shuler, Y. Tang, *J. Phys. Chem. B* **2004**, *108*, 12130–12140.
https://doi.org/10.1021/jp048773n

[15] K. E. Wardle, D. J. Henderson, R. L. Rowley, *Fluid Phase Equilibria* **2005**, *233*, 96–102.
https://doi.org/10.1016/j.fluid.2005.03.033

[16] X. An, H. Lei, Y. Lu, X. Xie, P. Wang, J. Liao, Z. Liang, B. Sun, Z. Wu, *Sci. Total Environment* **2023**, *890*, 164207.
https://doi.org/10.1016/j.scitotenv.2023.164207

[17] X. Jing, L. Zhou, S. Li, Y. Xu, Q. Liu, Z. Fu, *Chem. Papers* **2023**, *77*, 7457–7464.
https://doi.org/10.1007/s11696-023-03018-5

[18] F. Neese, F. Wennmohs, U. Becker, C. Riplinger, *J. Chem. Phys.* **2020**, *152*, 224108.
https://doi.org/10.1063/5.0004608

[19] F. Nees, *WIREs Computational Molecular Science* **2012**, *2*, 73–78. https://doi.org/10.1002/wcms.81

[20] J. G. Brandenburg, C. Bannwart, A. Hansen, S. Grimme, *J. Chem. Phys* **2018**, *148*, 64104.
https://doi.org/10.1063/1.5012601

[21] X. Jing, Q. Luo, X. Cui, Q. Wang, Y. Liu, Z. Fu, *J. Molecular Liquids* **2022**, *366*, 120237.
https://doi.org/10.1016/j.molliq.2022.120237

[22] M. J. Abraham, T. Murtola, R. Schulz, J. C. Smith, B. Hess, E. Lindahl, *SoftwareX* **2015**, *1*, 19–25.
https://doi.org/10.1016/j.softx.2015.06.001

[23] D. Van Der Spoel, E. Lindahl, B. Hess B, G. Groenhof, A. E. Mark, H. J. C. Berendsen, *J. Computational Chemistry* **2005**, *26*, 1701–1718.
https://doi.org/10.1002/jcc.20291

[24] J. Wang, R. M. Wolf, J. W. CaldwellP. A. Kollman, D. A. Case, *J. Computational Chemistry* **2004**, *25*, 1157–1174.
https://doi.org/10.1002/jcc.20035

[25] C. I. Bayly, P. Cieplak, W. Cornell, P. A. Kollman, *J. Phys. Chem.* **1993**, *97*, 10269–10280.
https://doi.org/10.1021/j100142a004

[26] T. Lu, F. Chen, F. *J. Computational Chemistry* **2012**, *33*, 580–592.
https://doi.org/10.1002/jcc.22885

[27] L. Martínez, R. Andrade, E. G. Birgin, J. M. Martinez, *J. Computational Chemistry* **2009**, *30*, 2157–2164.
https://doi.org/10.1002/jcc.21224

[28] S. Izadi, A. V. Onufriev, *J. Chem. Physics* **2016**, *145*, 74501. https://doi.org/10.1063/1.4960175

[29] G. Bussi, D. Donadio, M. Parrinello, *J. Chem. Physics* **2007**, *126*, 14101.
https://doi.org/10.1063/1.2408420

[30] T. Darden, D. York, L. Pedersen, *J. Chem. Physics* **1993**, *98*, 10089–10092.
https://doi.org/10.1063/1.464397

[31] W. Humphrey, A. Dalke, K. Schulten, *J. Molecular Graphics* **1996**, *14*, 33–38.
https://doi.org/10.1016/0263-7855(96)00018-5

[32] T. Lu, Q. Chen, *J. Computational Chemistry* **2022**, *43*, 539–555.
https://doi.org/10.1002/jcc.26812